Available online at www.sciencedirect.com
SCIENCE DIRECT
Polymer 46 (2005) 1169–1179
polymer
www.elsevier.com/locate/polymer

Aqueous heterophase polymerization of styrene—a study by means of multi-angle laser light scattering

Steffen Kozempel*, Klaus Tauer, Gudrun Rother

Max Planck Institute of Colloids and Interfaces, Am Mühlenberg, D-14476 Golm, Germany

Accepted 30 September 2004
Available online 8 December 2004

Abstract

An online multi-angle laser light scattering study of ab initio surfactant-free styrene emulsion polymerization reveals unexpected results regarding the development of the dispersity during the whole reaction starting from mixing styrene and water at reaction temperature. The experimentally observed change in the dispersity, which is an indirect measure of the average characteristic size of the colloidal objects, allows the identification of three characteristic intervals. During interval A the equilibration of styrene in water is characterized by the formation of styrene domains, which increase in number and size until an equilibrium state is reached. This means that there is virtually no homogeneous/molecular styrene in water solution but rather nanodroplets of about 200 nm in diameter (assuming spherical shape) are formed. During interval B, after initiation of the polymerization and particle formation, the dispersity increases again as the average size decreases and the number of scattering objects increases. The polymer particles suck up the monomer from the monomer nanodroplets, which leads to the disappearance of the nanodroplets and to a decrease in the average size. During interval C the average size increases again due to the predominantly growth of the polystyrene particles.

Keywords: Online multi-angle laser light scattering (MALLS); Emulsion polymerization; Particle nucleation

1. Introduction

Nucleation such as particle formation in heterophase polymerization is a process that is still not yet fully understood. The investigation of the very early stages of any reaction is experimentally very challenging. This is also true for heterophase polymerization where particle nucleation takes place at extremely low conversion after an apparently homogeneous pre-nucleation period. Exemplary [1], for surfactant-free polymerization of styrene initiated with 2.5 mM potassium peroxodisulfate (KPS) at 60 °C the pre-nucleation period has a duration of 431 s, nucleation takes place 432 s after initiator addition where a huge number of particles ($N_0 = 1.76 \times 10^{13}$ cm^{-3}) is formed with an average diameter of about 13 nm. Each of these particles consists at birth of about 7000 styrene units as maximum value (for the calculation the density of polystyrene was used and no end groups were considered). This is not an unrealistic number as the total number of styrene units inside particles (1.23×10^{17} cm^{-3}) is lower than the saturation concentration of styrene in the aqueous phase at 60 °C, which is about 3.06×10^{18} cm^{-3} [2]. From the total number of styrene units inside particles at nucleation follows that the minimum amount of polymer formed up to this moment is 2.13×10^{-5} g cm^{-3}. In subsequent studies a so-called Jumbo-effect was observed [3], which means that during the nucleation period surprisingly an increase in the transmission was observed for a certain period of time. This unusual effect, which was observed for styrene, methyl methacrylate, and vinyl acetate as monomer at reaction temperatures of 60 and 70 °C, is far from being understood at the moment. In order to shed light on the Jumbo-effect and particularly n the question how this effect is related to particle nucleation a study by means of time dependent multi-angle laser light scattering (MALLS)

* Corresponding author. Tel.: +49 331 567 9511; fax: +49 331 567 9512.
E-mail addresses: steffen.kozempel@mpikg.mpg.de (S. Kozempel), klaus.tauer@mpikg-golm.mpg.de (K. Tauer), gudrun.rother@mpikg.mpg.de (G. Rother).

0032-3861/$ - see front matter © 2004 Elsevier Ltd. All rights reserved.
doi:10.1016/j.polymer.2004.11.060

was started. This contribution describes for the first time the use of MALLS for online analysis of heterophase polymerizations. Two papers describing online time dependent static light scattering technique (TDSLS) to study solution polymerization processes have been published very recently. These results show that it is possible to use TDSLS to analyze polymerization processes [4,5]. The use of MALLS in the configuration that is available in our lab requires investigations at room temperature and hence, it is necessary to use a redox initiating system, which should be robust, reproducibly working, and allow a control of the polymerization rate so that it is possible to gain enough scattering data during the initial period of the polymerization. Therefore a redox initiator system of potassium peroxodisulfate and sodium metabisulfite as described in Ref. [6] was chosen and modified in accordance with the specific requirements. The formation of initiating species without consideration of side reactions takes place as shown by the equations in Scheme 1. Both the sulfate ion radical and the sulfonate ion radical can initiate polymerization [6]. Thus, this redox system leads at least to two, chemically different nucleating species, which means that at least two different kinds of end-groups (sulfonate and sulfate groups) can be expected in the polymer.

This contribution reports surprising results obtained with MALLS during the investigation of ab initio, surfactant-free heterophase polymerization of styrene at room temperature (25 °C) including the pre-reaction equilibration period that is, the establishment of an equilibrium styrene concentration in the continuous phase before adding the initiator system. The amazing results are experimentally confirmed and supported by ultraviolet spectroscopic measurements and polymerizations in an all-Teflon reactor equipped with online conductivity and transmission measurements as described in Ref. [7].

2. Experimental information

2.1. Materials

Styrene (from Sigma-Aldrich) was distilled under reduced pressure before use. The water for all experiments was taken from a Seral purification system (PURELAB Plus™) with a conductivity of 0.06 μS cm^{-1} and carefully degassed prior to use as described in Ref. [7]. Potassium peroxodisulfate (KPS) and sodium metabisulfite (SMBS) from Sigma-Aldrich were used as received.

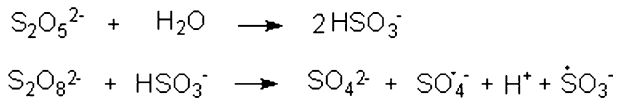

Scheme 1. Formation of initiating radicals by the redox couple persulfate/metabisulfite.

2.2. MALLS measurements, sensitivity, data acquisition and analysis

For the time dependent static light scattering studies the MALLS instrument DAWN EOS from Wyatt Technology Corporation (Santa Barbara, USA) equipped with a 30 mW GaAs laser (wavelength of 690 nm) was used. The original instrument is equipped with a flow cell for the use in chromatographic studies. The scattering intensity is measured simultaneously with an array of 18 photo detectors in an angle range between 22.5 and 147° around the cell. This arrangement allows the continuous registration of complete scattering curves. The equipment was modified as described in Ref. [8] essentially by using a toluene index matching bath (manufactured by Hellma, Germany) and cuvettes as scattering cells. The scattering cells are standard quartz glass cuvettes (Hellma, Germany) with a diameter of 20 mm and a height of 8 cm and hence, their volume is sufficiently large allow online monitoring of reactions carried out therein.

Wyatt offers a software package ASTRA, which collects and processes signals transmitted from the DAWN instrument to the computer. This program saves the data in a special file format. Calibration and normalization constants, scattering of the solvent and of the sample solution as well as the constants for data evaluation are incorporated. The data are processed to obtain the Rayleigh ratio $R(q)$ of the scattering intensity of the sample solution. The output is a chronology of scattering curves $R(q)/(Kc)$ versus q, where K is the contrast factor, c is the mass concentration of scattering species, $q=(4\pi/\lambda)\sin(\Theta/2)$ is the length of scattering vector, λ is the wavelength in the medium, and Θ is the scattering angle. A collection interval of 10 s yields six complete scattering curves per minute.

The measuring range of the DAWN EOS is limited by the saturation point of the photodetectors (10 V). Reduction of the amplification enlarges the range to 100 V, which corresponds at a scattering angle of 90° to 370 times the scattering of toluene (370 toluene units). The geometrical arrangement allows 520 toluene units at a scattering angle of 22.5°. Additional application of grey filters can further enhance the measuring range. During the experiments the maximum scattering was 290 and 200 toluene units at a scattering angle of 22.5 and 90°, respectively. The base line was determined with pure water transferred into the cuvette through a 0.2 μm syringe filter. The scattering of water is about 1/10 of toluene. The excess scattering of the reaction mixtures above water bounds the measuring range below.

A special software package LISA [9] was developed for a sophisticated analysis of the scattering curves, because interpretation with the traditional methods fails due to the strong angular dependence of the scattering curves in the case of larger scattering species. Special routines were written to convert the ASTRA ASCII exported data in a LISA readable form.

With LISA the data were analyzed by an improved

algorithm based on a fit procedure by theoretical model curves in a scaled representation [8–11] by plotting $\log R(q)/(Kc)$ versus $\log q$. The assignment of an experimental curve to an appropriate theoretical one allows getting information about the structure type and the polydispersity of the scattering system. The fit then provides the structural parameters M_w (the weight average of molar mass) and R_G (the radius of gyration). Knowing the polydispersity σ of the assumed logarithmic distribution function and supposing that the ensemble of scattering particles are spheres of homogenous density a corrected value of the sphere radius r_m and also the structural density ρ can be calculated. It is to emphasize that only under these conditions the relation $M_w=(4\pi/3)\rho r_m^3$ is valid. The polydispersity σ, the parameter of the used logarithmic distribution, corresponds for smaller values to the relative standard deviation. Furthermore, LISA also admits bimodal interpretations, what means a scattering equivalent fit with a model of two ensembles of scatterers, which are reflected in different sections of the scattering curve.

The size of the scattering species and the structure type (shape of the scattering species) determines the form of the scattering curves. The mass and the optical parameters of the substances affect the absolute value of $R(q)/(Kc)$. All parameters multiplicatively contained in $R(q)/(Kc)$ do not influence the shape of the scattering curve nor the interpretations with regard to the size. Therefore it will be possible to estimate particle sizes without knowing the refraction index increments (dn/dc) and the concentrations. Of course the procedure requires the applicability of the principles of light scattering in diluted systems. However, these conditions are fulfilled for the presented investigations as shown by the following considerations. The maximum styrene concentration applied during the experiments in the MALLS cuvette is less than 1 mg ml^{-1} of water and hence, the number of styrene particles (N) at complete conversion is 1.5×10^{13}, 1.8×10^{12}, and 2.3×10^{11} ml^{-1} of water for average particle sizes of 50, 100, and 200 nm, respectively. Considering the amount of styrene dissolved in water, which is about 0.18 mg ml^{-1} at 25 °C [2] the corresponding particle numbers are by about the factor of 5 lower. The latter values should correspond to the situation during the particle nucleation period of the polymerizations. According to experimental data obtained for electrostatically stabilized polystyrene particles with a diameter of about 100 nm the mean number of scattering events per photon (p_s) is given by $p_s=0.4\times10^{-12}$ N (ml^{-1}) [12]. This relation shows that especially during the initial period of the polymerization when the majority of the styrene is still unreacted on top of the aqueous phase multiple scattering is no issue. Moreover, for small particles the intensity of multiple scattering relative to that of single scattering scales with ND^6 [13]. Exemplarily, for $N<8.5\times10^{12}$ ml^{-1} of about 50 nm sized particles (charged stabilized polystyrene spheres) multiple scattering was small [14]. Note, the initial particle density after particle nucleation is in our experiments at least by a factor two lower. Additional evidence that multiple scattering, if it ever occurs, is only of minor importance comes from the following observations. Firstly, the concentration of the dispersions obtained hours after nucleation from the experiments in the MALLS cuvette is so low that it is impossible to determine the average particle size with standard dynamic light scattering equipment (Nicomp particle sizer, model 370, particle sizing systems, Santa Barbara, California, USA). Secondly, for the polymerizations in the Teflon reactor with online transmission and conductivity monitoring the transmission reaches only more than 1000 min after initiation a value of 89% (cf. data shown in Fig. 8), which according to results in Ref. [12] means p_s smaller than 1.

In conclusion, the polymerization experiments in the MALLS cuvette are carried out under conditions where multiple scattering is rather unlikely and thus, the time dependent investigations described in this study with multi-angle SLS should be valid.

2.3. Polymerization in the MALLS cuvette

The polymerizations were carried out in cylindrical Quartz cuvettes (Hellma, Germany) with an inner diameter of 18 mm closed with a PTFE stopper at 25 °C. If not otherwise stated the following procedure was employed. Deionized water (90 g) was degassed by boiling and vacuum treatment. During cooling at about 70 °C styrene (1.5 g) was added and the mixture was gently stirred (70 rpm) over a period of time of up to 5 h. This should ensure to start the polymerization with saturated styrene solutions in water. To this solution the redox initiator couple was added starting with 25 mM KPS solution (0.013 g in 2 ml of water) and followed by 50 mM SMBS solution (0.029 g in 3 ml of water). In a series of preparatory experiments it turned out that this initiator concentration allows the investigation of the initial period of the polymerization in the MALLS equipment with sufficiently high resolution. After stirring the reaction mixture for 1 min 10 ml were transferred through a syringe filter of 0.8 μm into the MALLS-cuvette. Note, this procedure ensures that no free styrene is transferred into the MALLS cuvette. After positioning the cuvette in the MALLS instrument an additional drop of styrene (0.007 g) was deposited on top of the solution through a syringe with a 0.45 μm filter. The MALLS-measurements were immediately started after these preparations.

2.4. Polymerization in the all Teflon reactor

For the sake of comparison polymerizations were also performed in an all-Teflon reactor equipped with online conductivity probe and transmission measurement (optical

path length of 9.8 cm) as described in Ref. [7]. The total reaction volume was 400 ml and the polymerization mixture was gently stirred with 70 rpm during the entire polymerizations.

2.5. UV measurements

UV measurements were carried out with an UVIKON 931 spectrometer (Kontron Instruments, UK) in the wavelength range between 310 and 190 nm in quartz cuvettes with an optical path length of 1 cm.

3. Results and discussions

Fig. 1(a) shows the development of the average size of the scattering objects as determined during a typical on line MALLS polymerization experiment where t'' denotes the time elapsed during the MALLS measurements.

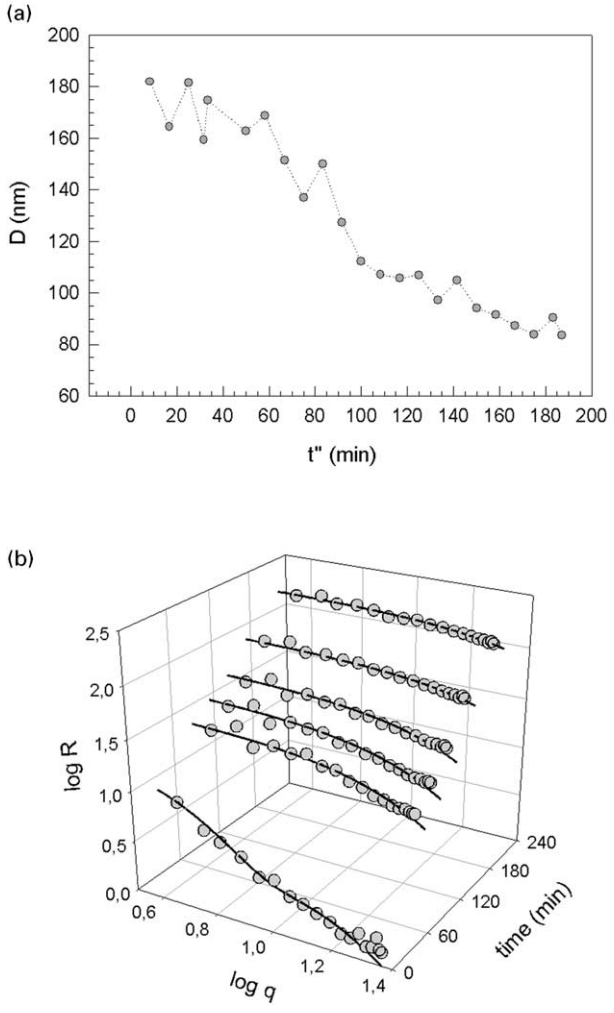

Fig. 1. (a) Average particle size as determined in a particular online MALLS experiments; at $t''=0$ the MALLS measurements were started (about 1 min after initiator addition to a saturated styrene in water solution). (b) Chronology of selected scattering curves ($\log R$ versus $\log q$) (R—Rayleigh ratio in arbitrary units) as obtained for polymerizations in the MALLS cuvette (symbols—experimental points, solid lines—adequate interpretation models).

This result is really surprising as it is in obvious contradiction to all experiences (cf. [15–17]) and former experimental data [1,7,18]. Instead of the observed continuous decrease in D starting from about 180 nm one would expect that the average particles size increases during the initial period of the polymerization.

Fig. 1(b) shows the corresponding experimental scattering curves (filled circles) recorded during such a run. The solid lines are the result of the analysis of the scattering curves with LISA using adequate interpretation models. These curves were obtained for spheres of homogenous density with a polydispersity $\sigma=0.3$ of an assumed logarithmic distribution. The good agreement between experimental and fitted curves proves the validity of the applied data interpretation procedure.

The curve at time zero in Fig. 1(b) shows the scattering behavior of a styrene in water solution after equilibration as it was obtained before the addition of the initiating system. Data interpretation for this scattering curve is successfully possible with the assumption of a bimodal size distribution consisting of spheres with a diameter of about $D_1=180$ nm for the bulk of the droplets and in the order of $D_2=800$ nm for the minor part (rough estimation results in less than 1 wt% of all scatterers). It is important to emphasize that the scattering of the styrene in water solution without initiator addition remains within the experimental error unchanged for several hours.

However, during the polymerization reaction the average size of the scattering objects decreases (indicated by the decreasing curvature of the scattering curves) as it is also shown in Fig. 1(a) whereas the number of scatterers increases (indicated by the increasing Rayleigh ratio, R).

These results, especially those obtained for the starting styrene in water solution, which appears optically transparent to the naked human eyes, induced investigations of the time development of the scattering behavior with slow diffusion of styrene that is, without any mixing. Under these conditions the saturation of water with styrene takes place by diffusion from top of the water phase through the interface.

Knowing the tremendous influence of dissolved gas on particle nucleation as described in Ref. [7,18] the evolution of the scattering behavior during the equilibration period that is, during the dissolution of styrene in either carefully degassed or gassed water without starting the polymerization, has been investigated. Again, these experiments showed surprising results, which finally opened the door to understand the results obtained for the polymerizing systems as shown in Fig. 1(a) and (b). The evolution of the scattering intensity during the dissolution of styrene in both non-degassed and degassed water is shown in Fig. 2(a) and (b), respectively. The scattering data were recorded after five drops of styrene were carefully placed on top of

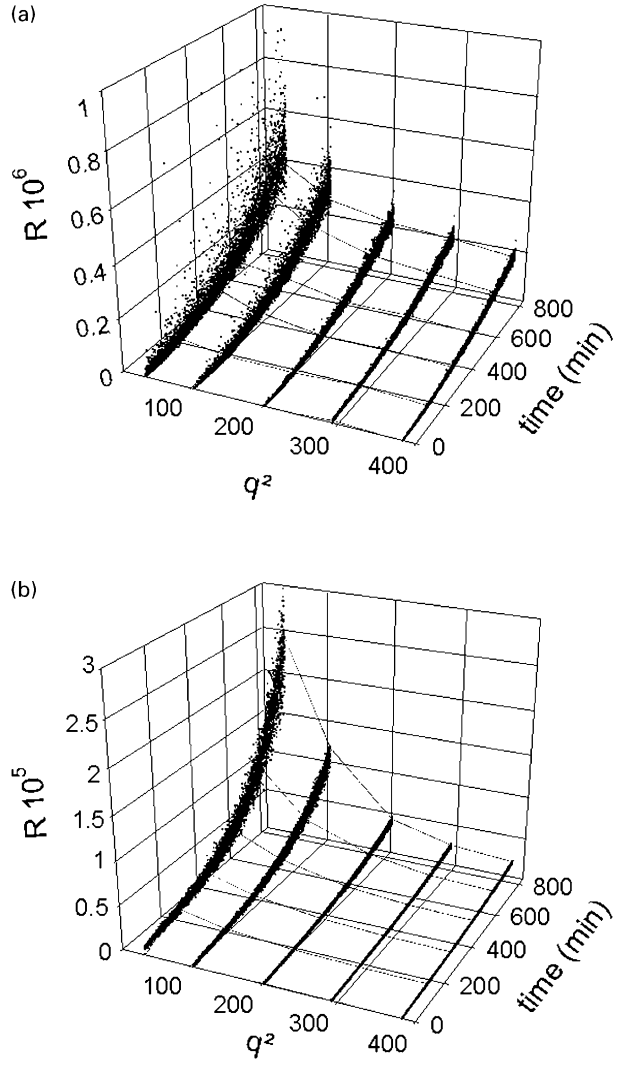

Fig. 2. (a) Evolution of the scattering intensities during the dissolution of styrene in gassed water for scattering angles of 28, 50, 72, 90, and 108°; time = 0 denotes the start of the MALLS measurement. (b) Evolution of the scattering intensities during the dissolution of styrene in carefully degassed water for scattering angles of 28, 50, 72, 90, and 108°; time = 0 denotes the start of the MALLS measurement.

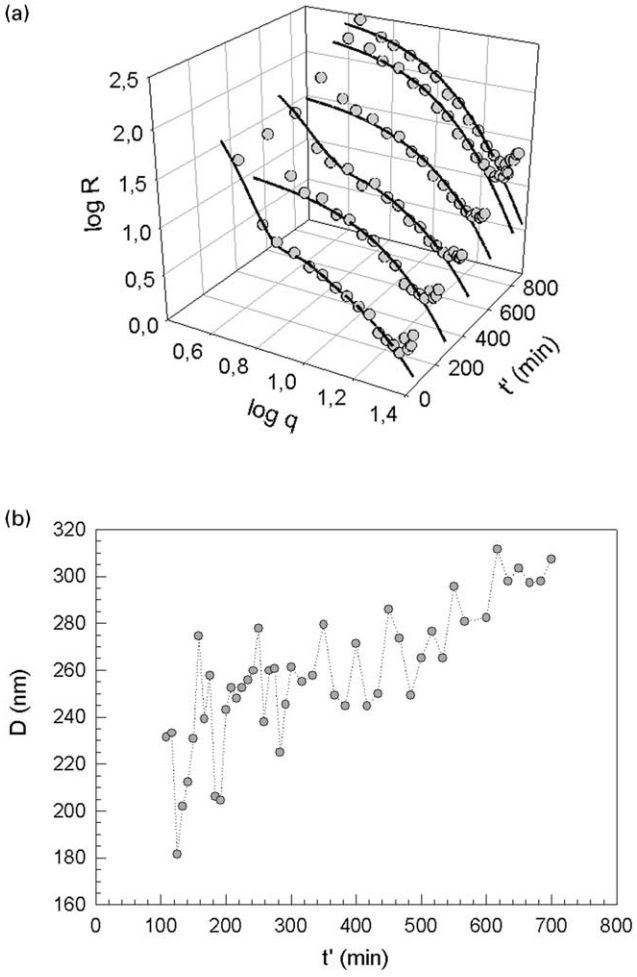

Fig. 3. (a) Development of the scattering curves during diffusion of styrene into water; chronology of selected scattering curves log R versus log q (R—Rayleigh ratio in arbitrary units), symbols—experimental points, solid lines—adequate interpretation models. (b) Increase in the average size of the scattering objects during the dissolution of styrene in carefully degassed water.

10 ml of pure water in the MALLS cuvette. The quantitative difference between both sets of experiments is amazing (the Y-axis in Fig. 2(a) for the gassed water is by a factor of 30 stretched compared with that in Fig. 2(b)). In the period of time considered (t') the scattering intensity of the experiments with non-degassed water increases only slightly above the scattering value obtained for pure water. Nevertheless, the data show a slow and continuous increase even if the excess scattering is too low to calculate average sizes.

On the contrary, the excess scattering during the diffusion of styrene into carefully degassed water becomes so high that an evaluation of the data is possible as exemplary shown in Fig. 3(a) (scattering curves) and Fig. 3(b) (average size).

After about 100 min the scattering intensity is high enough to allow quantitative data evaluation. Again, the interpretation was carried out with models of spheres of homogenous density (solid lines). The first and the third curves along the time axis were fitted with models assuming bimodal size distributions. These data clearly show that the bimodality decreases with time. The scattering curve after about 900 min can be interpreted assuming a monomodal distribution. A closer inspection reveals that also the portion of larger droplets (about 1200 nm in diameter) decreases with time. While it is substantially for the scattering curve measured after 110 min it decreases to about 10% in the particle number density for the curve obtained after 7 h. In the same time the average size of the larger droplets decreases to about 1000 nm in diameter. For the model interpretations of curves 2 and 4 after about 270 and 600 min, respectively, only the dominating part of the smaller scatterers was considered (logarithmical distribution with polydispersity $\sigma = 0.3$).

Fig. 3(b) shows the change of the estimated average sizes of the droplet fraction dominating the scattering behavior during the first 12 h. The average droplet size reaches a value of about 600 nm after 25 h with slightly increasing polydispersity ($\sigma = 0.4$). After about 33 h a plateau is of both the scattering intensity and the average droplet size is seemingly reached.

The evaluation of the scattering data in Fig. 3(a) reveals that not only the size of dominant scatterers increases but also their number. Quantification regarding the number of drops is not possible as the adequate result of the scattering experiments, which is the product cM_w, cannot be resolved. However, the assumption of constant density allows these qualitative conclusions.

The behavior as depicted in Figs. 2 and 3 is typical and has been repeatedly observed. It is to note that the aqueous phase of the styrene–water mixture appears absolutely transparent by visual inspection. Furthermore, the scattering intensity of these samples is too low for a commercial light scattering device such as the Nicomp particle sizer (model 370) as the countrate is smaller than 20 kHz. Despite all the statistical scatter of the experimental data the MALLS results show that styrene dissolves not only molecularly in water but also forms aggregates or droplets. These aggregates or droplets might be considered in a physical equivalent way as concentration fluctuations indicating regions of supersaturation of styrene in water. Consequently, on the one hand these data arise questions regarding the equilibrium concentration of styrene in water and on the other hand regarding the general physical state of a 'styrene in water solution'. These points are of importance for all kinetic considerations of heterophase polymerizations.

In order to compare the scattering curve at time zero as shown in Fig. 1(b) with the data shown in Fig. 3(a) and (b) it is to emphasize that both data sets refer to styrene in water solutions prepared in a different way. The former illustrates the situation after mechanical mixing styrene and water as described in the experimental part and shows a constant scattering behavior over several hours whereas the latter curves describe the situation during diffusion of styrene into water as purely thermodynamically driven process.

The conclusions drawn from the MALLS experiments are basically supported by results obtained with UV spectroscopy (Fig. 4(a) and (b). The UV spectra of styrene in water show especially during the first 17 min of the dissolution process strong fluctuations regarding both the shape and the band intensity (cf. Fig. 4(a)). After about 50 min the absorption of styrene is so high that the limit of the capability of the spectrometer is reached especially for the band at about 200 nm. Despite the scatter of the absorption spectra at short times the data clearly show that styrene diffuses from top of the water layer into the volume. There might be at least two reasons responsible for the observed changes in the absorption behavior at the beginning. Firstly, concentration fluctuations due to the slow diffusion of styrene from the top of the water layer into

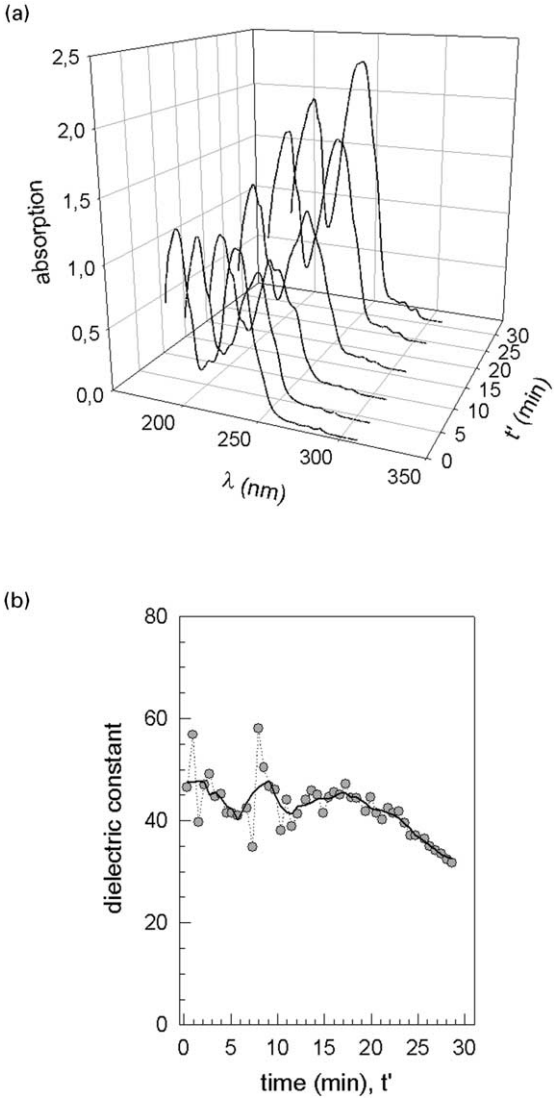

Fig. 4. (a) UV spectra recorded during the early stages of the dissolution of styrene in carefully degassed water. (b) Change of the dielectric constant of the styrene microenvironment calculated from the UV spectra during the dissolution of styrene in carefully degassed water; the dielectric constant was calculated ratio of the absorption intensity at 207 and 247.5 nm according to [19].

the volume of the cuvette passed from the light beam. Secondly, if styrene aggregates or even droplets are formed scattering effects may contribute to the weakening of the light intensity additionally to absorption.

UV spectroscopy is a useful tool to examine the state of solvation or the micro-environment of the absorbing species. Exemplary, the intensity ratio of the absorption bands at ~210 and ~240 nm can be used to get information about the polarity and the dielectric constant in the environment of the absorbing styrene molecules [19]. The data depicted in Fig. 4(b) show that during the dissolution of styrene in water at times longer than about 17 min the dielectric constant and hence also the polarity of the microenvironment decreases. Despite all scatter these

data also clearly show that the dielectric constant is from the beginning much lower than the value of water (78.5). This fact might lead to the conclusion that there is at no time a molecular solution of styrene in water but rather only aggregates, which subsequently grow larger in size as also observed in the MALLS experiments. Values of the dielectric constants below 30 estimated at longer times as shown in Fig. 4(b) have also been obtained for styrene solubilized in micelles [19,20]. In conclusion, of this part, the UV-spectroscopic data support the results of the MALLS data regarding the nature of a styrene in water solution. Both experiments suggest that in a styrene-in-water solution the styrene molecules exist not only molecularly dissolved and solvated by water molecules. At least a part of them is aggregated and should be present in the form of nanodroplets. This assumption fits fairly into the picture that a saturated solution might be considered to be situated in a phase diagram at the border between the single phase and the two phase region of the mixture. Thus, already slight changes in the local physical parameters such as temperature and composition can cause the system to fluctuate between both regions in the phase diagram.

The supposition of nanodroplets in neat styrene in water solutions arises immediately the question concerning the stabilization of these styrene droplets in the absence of any surfactant. One possibility to explain the stability of the nanodroplets might be that they gain enough entropy compared to the bulk phase. The difference between gassed and degassed water as shown in Fig. 2 suggests that the effect described here might be of similar origin as the striking differences observed regarding the stability between aerated and evacuated emulsions as described in Ref. [21]. These authors found that emulsions containing dissolved gas separated completely within minutes after preparation whereas the degassed counterparts remained stable for hours. On the one hand it has been suggested that hydrophobic surfaces are favorable places for the adsorption of dissolved (hydrophobic) gases [22] and on the other hand there is experimental evidence that a remarkable negative excess of water exists in contact with hydrophobic surfaces [23]. Recently a theory has been developed describing the solvation of differently sized objects in water indicating that the water density around larger objects is essentially that of water vapor or in other words that there is no hydrogen bonding between water and larger hydrophobic units and hence, the density of water molecules vanishes and excluded volume regions are generated [24]. This kind of hydrophobic effect that separates hydrophobic groups from water appears only when the local concentration of the hydrophobic parts is above a certain threshold large enough to induce drying. It is to point out that this phenomenon is not influencing the water structure near either small non-polar or larger polar units. Considering all these results one may conclude that the stability of the styrene droplets in mixtures with degassed water as observed in the present study is caused by water depletion layers, which should be physically equivalent to adsorbed layers of residual basically hydrophobic gas molecules or also might be considered as precursor layers for nanobubbles [25]. The gas layers or the nanobubbles can be stabilized even in the neat styrene–water system by selective adsorption of ions, very likely hydroxyl ions, providing electrostatic stabilization to the gas bubbles as discussed in Ref. [26]. However, if either the concentration of dissolved gas is too large or the concentration of droplets is too high enhanced droplet coalescence might occur. This is similar as during floatation where nanobubbles adhering to the surfaces cause the rupture of wetting films separating the particles [27,28]. Further support comes from direct force measurements with an atomic force microscope where attractive forces have been measured on the one hand between macroscopic hydrophobic surfaces [25,29–32] but on the other hand also between polystyrene particles with diameters between 1.8 and 6 μm mediated by nanobubbles [33,34]. These are really long-range attractive forces starting at separation distances up to 400 nm. Furthermore, there is clear experimental evidence that this range depends on the gas concentration in the continuous phase in a way that it decreases when the amount of dissolved gas in water is reduced [25,30–33].

It has been experimentally proven that the reproducibility of ab initio emulsion polymerizations, especially during the particle nucleation period, is considerably improved if carefully degassed water was used instead of gas-saturated water even if nitrogen was used and not just air [7]. Obviously, dissolved gas molecules, aggregates, or nanobubbles tremendously influence the particle nucleation during heterophase polymerizations and hence, the reproducibility of the whole process.

The scattering curves shown in Fig. 1(b) refer only to the initial part of the polymerization where particle nucleation takes place as indicated by the decrease in the average size of the scattering objects. This decrease in the average size is caused by an overlay of the styrene droplets and the polymer particles formed after initiator addition. About 200 min after initiator addition the average size starts to increase, which indicates ceasing particle nucleation and the beginning of predominant particle growth. Scattering curves during this stage of the reaction are exemplarily put together in Fig. 5 where again the solid lines are the relevant theoretical model curves for spheres (polydispersity $\sigma = 0.3$). The curvature of the scattering curves increases with time which means that the scattering objects grow in size. The average diameter of scatterers increases from $D \approx 100$ nm after 240 min (scattering curve 1) to $D \approx 145$ nm after 800 min (scattering curve 8). After this time the particle size stays almost constant $D \approx 150$ nm (scattering curves 9–12).

Summarizing the above experimental results, the colloidal state, especially the dispersity, during an ab initio surfactant-free emulsion polymerization changes as shown in Fig. 6. The time axis in this graph is arbitrary ($t' + t''$) as defined above but the particular time slots during the

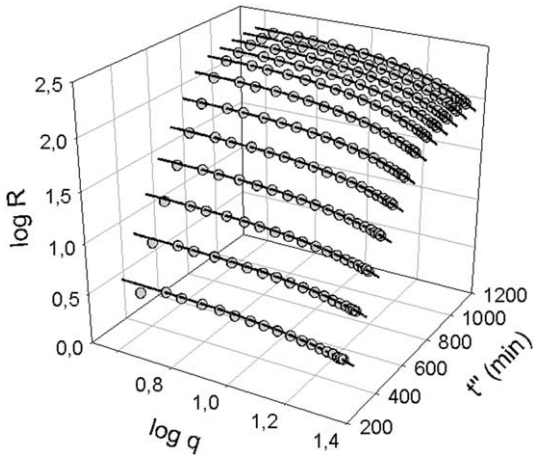

Fig. 5. Scattering curves during predominant particle growth (interval C); curve 1 and curve 12 after 240 and 1120 min, respectively; symbols—experimental points, solid lines—adequate interpretation models; time after the addition of initiator.

intervals (A, B and C) and the corresponding data points are real. This overall course as observed in the online MALLS experiments is really astonishing as it contradicts common expectations and former experiments. Based on former experimental data on particle nucleation [1,7,18] one would expect an increase in the average size after nucleation as indicated by the dashed line in Fig. 6.

Stage A represents the situation after the addition of the styrene monomer, that is, the dissolution of styrene in water accompanied by the formation of nanodroplets. After initiator addition and the pre-nucleation period particle formation takes place. During interval B, which is the particle nucleation period, the dispersity of the reaction system is governed by the coexistence of styrene nanodroplets and particles (some of them practically in the 'status nascendi'). After nucleation the particles suck up the monomer from the droplets and grow. The formation of polymer particles and their swelling with monomer leads to a net decrease in the average size describing an increasing

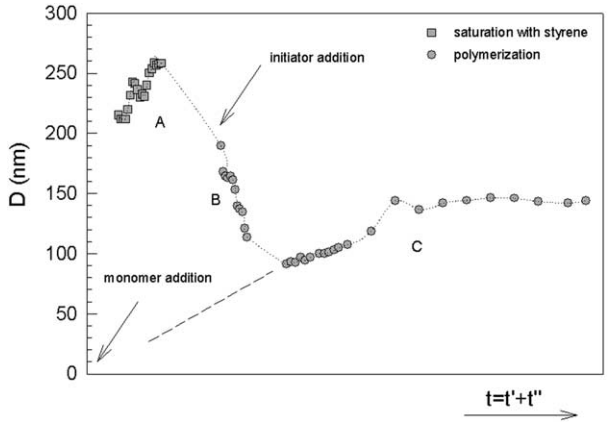

Fig. 6. Overall course of the dispersity during an ab initio surfactant-free emulsion polymerization of styrene expressed by means of the average size of the colloidal objects as determined by online MALLS measurements.

dispersity of the colloidal state. The qualitative analysis of the scattering curves as discussed in context with Figs. 3(a) and 5 shows that the number of scattering objects increases during the whole interval B and also during the beginning of interval C (up to about 800 min of the data in Fig. 5). Lasting polymerization during interval C leads to the disappearance of the neat styrene nanodroplets and to the stop of the particle growth. The size of the monomer swollen particles should decrease with increasing conversion after the disappearance of the monomer nanodroplets provided the stability of the particles is high enough to avoid coagulation. This might not necessarily be the case as the ionic strength with the redox initiator system is quite high (2.1×10^{-2} M). As the last stage of the polymerization was not the primary aim of these investigations only a few experiments have been carried out long enough to reach conversions clearly above 80%. In some cases a slight decrease of about 2–3 nm in the average diameter was observed, which, however, is with in the range of the reproducibility. The expected decrease in the average diameter from saturatedly swollen to completely polymerized particles is for a 150 nm swollen particle about 3.7 nm in diameter, which is clearly within the experimental uncertainty.

The new results discussed here made it necessary to repeat former polymerization experiments performed in the all-Teflon reactor as at that time no attention was paid to the duration of the equilibration period after styrene addition. Immediately before initiator addition the transmission was reset to 100% [3,7] and the polymerizations were started at different times after styrene addition (between 0.5 and 3 h). However, there was always observed a slight increase in transmittance ($\sim$0.5%) during nucleation, which was called Jumbo effect by the authors (cf. Fig. 7 and 8). In order to check whether the special features of these polymerizations, such as the Jumbo effect, are influenced by the duration of the styrene equilibration period some experiments were repeated at 70 °C. In these the styrene was allowed to equilibrate 3 h under reaction conditions (70 °C; 70 rpm) before KPS addition. The data of a particular polymerization are depicted in Fig. 7. These data represent also a record of the whole polymerization process starting from bringing water and styrene in contact at reaction temperature. For this particular run about 15 min after styrene addition the transmission starts to decrease from 100% and reaches after about 2.5 h a constant value of $\sim$91%. This decrease in the transmission is attributed to the scattering of the styrene droplets formed during the equilibration period. Again during the first experiments [7,18] the transmission was reset to 100% immediately before initiator addition as the peculiarities of a styrene in water solution were not known.

The transmission measurements are carried out at a wavelength of 546 nm where no absorption of styrene takes place but only light scattering can be observed. It is to note here that, although to different extents, the decrease in the

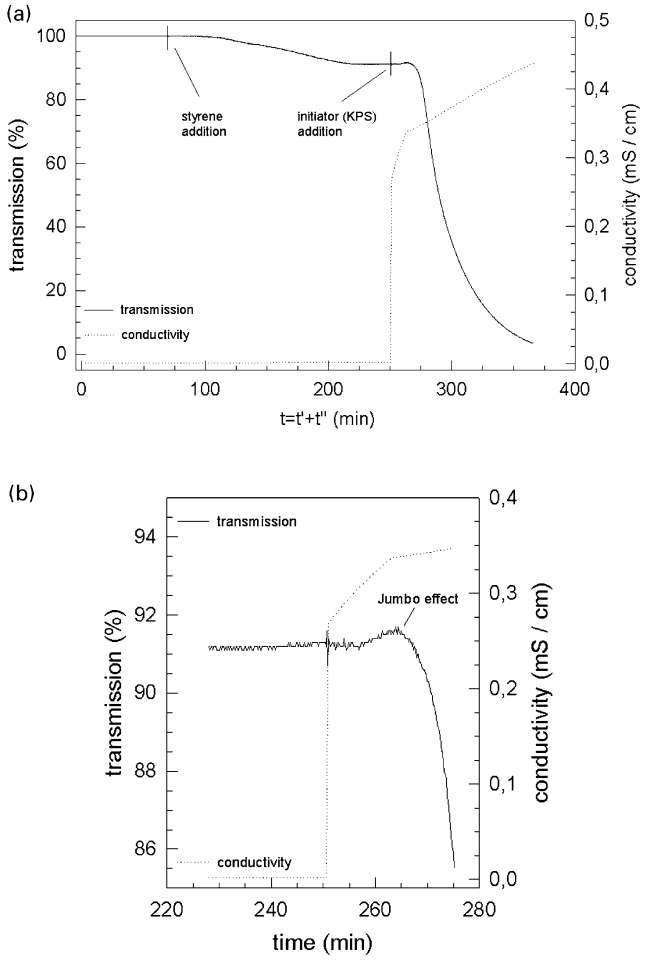

Fig. 7. (a) Online monitoring transmission and conductivity during an ab initio surfactant-free styrene emulsion polymerization in the all-Teflon reactor as described in Ref. [7] starting before styrene addition to water at reaction temperature (70 °C); 400 g of water, 3.3 g of styrene, 0.054 g of KPS. (b) Magnification of the changes during the particle nucleation period.

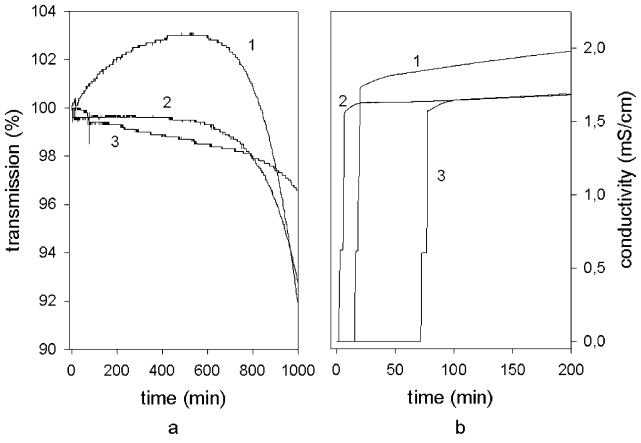

Fig. 8. Online monitoring transmission and conductivity during an ab initio surfactant-free styrene emulsion polymerization in the all-Teflon reactor as described in Ref. [7] starting before styrene addition to water at reaction temperature (25 °C); 400 g of water, 3.3 g of styrene, 0.216 g of KPS, 0.456 g of MBS; 1, 2, 3 represent three different runs representative for the various features observed.

transmission during the styrene equilibration period was observed in any experiment at 70 °C (40 single runs) whereas it was practically not to detect for polymerizations at 25 °C where admittedly up to now only about 10 experiments have been carried out.

Nevertheless, this observation is in accordance with an increased solubility of styrene in water at higher temperatures [2], which might cause the formation of either larger or a higher concentration of nanodroplets. After 3 h of styrene equilibration 10 ml of aqueous KPS solution (0.054 g of KPS) were injected to start the polymerization. An equilibration period of 3 h was supposed to be sufficiently long, which is supported by the fact that the transmittance does not change anymore. The bend in the conductivity curve, which indicates the appearance of the first particles [1,3,7,18], occurs 13.4 min after initiation. The data depicted in Fig. 7 clearly show a pronounced Jumbo-effect during the nucleation period as it was also the case in the former experiments [3].

Thus, it is clear that the duration of the equilibration period of styrene in water (Δt_{equ}) has virtually no influence on the appearance of the characteristic features (bend in conductivity and Jumbo-effect of the transmission curve). However, the quantitative evaluation reveals that there is an influence of Δt_{equ} on both the duration of the pre-nucleation period (Δt_{pn}) and the average particle size (D) at the end of the polymerization (transmission less than 10%). For instance, in one set of experiments (28 single runs) Δi_{equ} varied between 20 and 60 min Δt_{pn} and D was 17.2 ± 5 min and 118.2 ± 18 nm, respectively. On the contrary, in a second series (12 single runs) when Δt_{equ} was kept always 3 h, Δt_{pn} and D was 13.1 ± 1 min and 81.5 ± 5 nm, respectively. These characteristic data are clearly different and proving the enormous influence of the physical state of the monomer in the continuous water phase on particle nucleation.

The monomer nanodroplets obviously serve only as monomer reservoir supplying it due to its small size very efficiently to the reaction loci but not being itself the locus of initiation. There is no hint in any of our experiments that final particles in the size range of the nanodroplets (about 200 nm or larger) are formed. Furthermore, longer Δt_{equ} cause smaller final particles which can be explained with a higher oligomer concentration during the pre-nucleation period leading to the nucleation of a larger number but finally smaller particles according to the aggregative nucleation theory where the supersaturation is critical for the nucleation process [18,35].

The situation regarding the Jumbo-effect changes for the polymerizations at 25 °C as it is illustrated by the data put together in Fig. 8(a). The curves 1, 2, and 3 are representative for the different behavior that has been observed. Curve 1, 2, and 3 is representative for 30, 20, and 50% of the experiments carried out so far, respectively. The

important experimental fact is, that compared with the polymerizations at higher temperatures, where in any single run the Jumbo-effect was observed, it was detected for only 50% of the runs at 25 °C. Moreover, if the Jumbo-effect occurs the increase in the transmission is either up to 3% (case 1 in Fig. 8(a)) or less than 1% (case 2 in Fig. 8(a)). The latter magnitude is also observed for higher polymerization temperatures. In any case the duration of the Jumbo-effect is much longer at lower temperatures. This experimental observation indicates also a longer duration of the nucleation period (cf. Figs. 7 and 8). However, in 50% of the runs at 25 °C no Jumbo-effect was observed and the transmission started to decrease after the occurrence of the bend in the conductivity curve, which indicates the onset of particle nucleation [7,18].

The different behavior in dependence on the polymerization temperatures might be qualitatively explained within the frame of the classical nucleation theory. Accordingly, before nucleation can occur a activation free energy barrier has to be surmounted (ΔG^*) [36]. The rate of nucleation (J) is given by the following relation: $J \propto \exp(-\Delta G^*/k_B T)$ with $\Delta G^* \sigma^3 v^2/(k_B T \ln S)^2$ where σ is the interfacial tension nucleus to water, $k_B T$ is the thermal energy, S is the supersaturation (ratio concentration to solubility of the nucleating species), and v is the molar volume of the nucleating species. These relations reveal a strong dependence of the rate of nucleation on the temperature that is, J decreases with decreasing temperature. The influence of the temperature on ΔG^* is not easy to predict as σ, S, and v are also temperature-dependent. Generally, for any process the rate of nucleation is prone to scatter as the exponential dependence on ΔG^* makes it extremely sensitive to many factors such as already slight changes in the thermodynamic conditions as well as intermolecular potentials and traces of impurities. Even for the seemingly simple process of freezing water a huge scatter of the nucleation data has been observed [37]. The above results point to an enhanced scattering during the nucleation period at room temperature, which means that the activation free energy should be decreased at lower temperatures [37]. This is a hint that the temperature dependence of ΔG^* is determined by the temperature dependence of the supersaturation as the interfacial tension increases with decreasing temperature [3]. An increase in the supersaturation is not unrealistic as the solubility of the nucleating oligomers in water might very likely be reduced at lower temperature.

Finally, the question remains to consider why there is obviously no polymerization observed inside the nanodroplets. It sounds a logic explanation that the hydrophobic gas or bubble layer surrounding the styrene droplets (or the depletion zone of water molecules) prevents the entry of hydrophilic radicals very efficiently but allows the diffusion of the hydrophobic monomer molecules into the water phase. It is to note that the situation is completely different for surfactant-stabilized droplets where the hydrophilic interface does not favor the formation of hydrophobic gas layers and depletion zones of water molecules and hence allows the entry of radicals from the water phase.

4. Conclusions

The results presented in this study show, that the question regarding the concentration and the solution state of styrene in water at the beginning of a surfactant-free emulsion polymerization, that appears as extremely simple, in contrast turned out to be extremely complicated. As the solution state of styrene in water is not only, if so ever, molecularly dispersed its deeper investigation is of considerable importance for a better understanding regarding all aspects of ab initio aqueous heterophase polymerizations.

Furthermore, the present study reveals the necessity for the heterophase polymer chemists to consider aspects of modern physical chemistry, and particularly colloid chemistry, even if this necessitates a step away from easier, classical explanations that fail even qualitatively to describe the experimental results.

Based on the new insight gained in this experimental study the Jumbo-effect might be explained in the following way. The monomer consumption during the pre-nucleation stage outside the nanodroplets in the continuous phase causes shrinkage of the styrene nanodroplets, which might lead to an increase in the transmission. But this is only a hypothesis, which needs further experimental verification or refutation.

In a paper that was published and came to our attention after the submission of the manuscript due to the comments of one referee, Yamamoto et al. conclude that during the initial state of surfactant-free styrene emulsion polymerization particles are nucleated by two different mechanisms [38]. The first nucleation process proposed in this paper seemingly supports our findings as the authors conclude that monomer drops in the sub-micrometer size range formed by breakup from the monomer reservoir. On the contrary to our results, Yamamoto et al. [38] found evidence that the nanodroplets might be the first but minor locus of polymerization before the majority of particles is nucleated via aggregation of oligomers.

Acknowledgements

The authors thank the Max Planck Society and particularly the Max Planck Institute of Colloids and Interfaces, Department of Colloid Chemistry for financial support. Technical assistance given by Mrs. U. Lubahn and Mrs. S. Pirok is gratefully acknowledged.

References

[1] Tauer K, Deckwer R, Kühn I, Schellenberg C. Colloid Polym Sci 1999;277(7):607–26.

[2] Lane WH. Ind Eng Chem-Anal Ed 1946;18(5):295–6.
[3] Tauer K, Padtberg K, Dessy C. On-line monitoring of emusion polymerization. In: Daniels ES, Sudol ED, El-Aasser MS, editors. Polymer colloids–science and technology of latex systems, 2001. p. 93–112.
[4] Alb AM, Mignard E, Drenski MF, Reed WF. Macromolecules 2004; 37(7):2578–87.
[5] Drenski MF, Reed WF. J Appl Polym Sci 2004;92(4):2724–32.
[6] Ghosh P, Chadha SC, Palit SR. J Polym Sci Part A-General Pap 1964; 2(10P):4441–51.
[7] Kühn I, Tauer K. Macromolecules 1995;28:8122–8.
[8] Dautzenberg H, Rother G. Macromol Chem Phys 2004;205(1): 114–21.
[9] Rother G. Macromol Sympos 2000;162:45–61.
[10] Dautzenberg H, Rother G. J Polym Sci Part B-Polym Phys 1988; 26(2):353–66.
[11] Dautzenberg H, Rother G. Makromol Chem-Macromol Sympos 1992; 61:94–113.
[12] Gruner F, Lehmann W. J Phys-Math General 1980;13(6):2155–70.
[13] Pusey PN, Tough RJA. Particle interactions. In: Pecora P, editor. Dynamic light scattering. New York: Plenum Press; 1985. p. 85–179.
[14] Brown JC, Pusey PN, Goodwin JW, Ottewill RH. J Phys-Math General 1975;8(5):664–82.
[15] Gilbert RG. Emulsion polymerization—a mechanistic approach. London: Academic Press; 1995.
[16] El-Aasser MS, Sudol ED. Features of emulsion polymerization. In: Lovell PA, El-Aasser MS, editors. Emulsion polymerization and emulsion polymers. Wiley: Chichester; 1997. p. 37–58.
[17] Fitch R. Polymer colloids: a comprehensive introduction. San Diego: Academic Press; 1997.
[18] Tauer K, Kühn I. Particle nucleation at the beginning of emulsion polymerization. In: Asua JM, editor. Polymeric dispersions: principles and applications. Dordrecht: Kluwer Academic Publishers; 1997. p. 46–65.
[19] Schulz PC, Minardi RM, Vuano B. Colloid Polym Sci 1998;276(3): 278–81.
[20] Becerra F, Soltero JFA, Puig JE, Schulz PC, Esquena J, Solans C. Colloid Polym Sci 2003;282(2):103–9.
[21] Karaman ME, Ninham BW, Pashley RM. J Phys Chem 1996;100(38): 15503–7.
[22] Craig VSJ, Ninham BW, Pashley RM. Nature 1993;364(6435):317–9.
[23] Ash SG, Findenegg GH. Spec Discuss Faraday Soc 1970;1:105–11.
[24] Lum K, Chandler D, Weeks JD. J Phys Chem B 1999;103(22): 4570–7.
[25] Steitz R, Gutberlet T, Hauss T, Klosgen B, Krastev R, Schemmel S, Simonsen AC, Findenegg GH. Langmuir 2003;19(6):2409–18.
[26] Bunkin NF, Bunkin FV. Zhurnal Eksperimentalnoi I Teoreticheskoi Fiziki 1992;101(2):512–27.
[27] Stockelhuber KW, Radoev B, Wenger A, Schulze HJ. Langmuir 2004; 20(1):164–8.
[28] Schulze HJ, Stockelhuber KW, Wenger A. Colloid Surf-Physicochem Eng Asp 2001;192(1–3):61–72.
[29] Attard P, Moody MP, Tyrrell JWG. Phys-Stat Mech Appl 2002; 314(1–4):696–705.
[30] Yang JW, Duan JM, Fornasiero D, Ralston J. J Phys Chem B 2003; 107(25):6139–47.
[31] Ralston J, Fornasiero D, Mishchuk N. Colloid Surf-Physicochem Eng Asp 2001;192(1–3):39–51.
[32] Wood J, Sharma R. Langmuir 1995;11(12):4797–802.
[33] Considine RF, Hayes RA, Horn RG. Langmuir 1999;15(5):1657–9.
[34] Vinogradova OI, Yakubov GE, Butt HJ. J Chem Phys 2001;114(18): 8124–31.
[35] Tauer K, Kühn I. Macromolecules 1995;28:2236–9.
[36] Laaksonen A, Talanquer V, Oxtoby DW. Annu Rev Phys Chem 1995; 46:489–524.
[37] Heneghan AF, Wilson PW, Wang GM, Haymet ADJ. J Chem Phys 2001;115(16):7599–608.
[38] Yamamoto T, Kanda Y, Higashitani K. Langmuir 2004;20(11): 4400–5.